Graphene Oxide Dispersed Carbon Nanotube and Iron Phthalocyanine Composite Modified Electrode for the Electrocatalytic Determination of Hydrazine

Veerappan Mani, A.T. Ezhil Vilian, Shen-Ming Chen[*]

Department of Chemical Engineering and Biotechnology, National Taipei University of Technology, No.1, Section 3, Chung-Hsiao East Road , Taipei 106, Taiwan (R.O.C).
[*]E-mail: smchen78@ms15.hinet.net

We have synthesized graphene dispersed carbon nanotube and Iron phthalocyanine composite (GO-CNT-FePc) and successfully employed it for the electrochemical determination of hydrazine. The synthesized composite has been well characterized by scanning electron microscope (SEM), transmission emission microscopy (TEM) and energy-dispersive X-ray (EDX) spectroscopy. GO-CNT-FePc modified glassy carbon electrode (GCE) was prepared and its electrochemical behavior has been accessed by cyclic voltammetry. GO-CNT-FePc modified GCE exhibited highly enhanced hydrazine oxidation peak current at appreciably lower potential of +0.18 V. Therefore, the prepared GO-CNT-FePc modified GCE was demonstrated for the sensing of hydrazine by amperometry. The constructed GO-CNT-FePc modified electrode detects hydrazine in a wide linear range of 5×10^{-7}-8.35×10^{-5} M, with very low detection limit of 9.3×10^{-8} M. The sensor exhibited an acceptable repeatability and reproducibility. The excellent recoveries achieved for the hydrazine determination in various water samples reveal the promising practicality of the sensor.

1. INTRODUCTION

Hydrazine is a powerful redcuing agent and owing to its extreme toxicity, it shows severe carcinogenic and mutagenic effects [1-3]. Also, it have significant contribution to industrial and pharmaceutical applications in diverse areas such as rocket propellant, insecticides and explosives [4]. Therefore the sensitive determination of hydrazine is of great importance. Though a variety of methods available for the determinaion of hydrazine [5-7], electrochemical methods are simple, sensitive and of low cost [8]. On the other hand, in electrochemical methods bare electrodes encompass high

overpotential and often suffer from fouling effects. To overcome this issue, numerous chemically modified electrodes were prepared for the electrochemical determination of hydrazine. For example, some of the previous literature reports includes, polyaniline/graphene composite [1], Vitamin B12-multi-walled carbon nanotubes (MWCNT) composite film [4], cobalt hexacyanoferrate modified MWCNT/graphite composite electrode [9], high specific surface area graphene [10], ZnO on single walled carbon nanotube (SWCNT) [11], zirconium hexacyanoferrate film-bimetallic Au–Pt inorganic–organic hybrid nanocomposite [12], Nanocrystalline graphite-like pyrolytic carbon film electrode [13] and carbon nanotube (CNT) supported platinum nanoparticles [14]. CNT is an emerging material for the modified electrodes because of its unique properties such as large surface area and high electron communication [15-22].

Graphene oxide (GO), oxygenated derivative of graphene is an amphiphilic molecule containing various fuctional groups such as epoxy, hydroxyl and carboxyl groups on its surface. [23, 24]. GO is an excellent dispersent for CNT, through non-covalent π-π stacking interactions between its hydrophobic domain and sidewalls of CNT. Moreover, the dispersion is highly stable for more than 6 months without any precipitation [25, 26]. Graphene oxide dispersed Carbon nanotube (GO-CNT) have been extensively studied for its outstanding properties in various fields such as dye sensitised solar cells [27], supercapacitors [28], proton exchange membrane fuel cell [29], biofuel cells [30], sensors [31] and biosensors [32]. In our previous report [32] we briefly elucidated the preparation and characterisation of GO-CNT composite. Iron phathalocyanine (FePc) is one of the extensively studied phatholocyanine owing to its excellent electrocatalytic ability [33]. It has been proved that CNT-Phathalocyanine composite can be prepared through non-covent supramolecular interactions [34]. Similarly, GO-Phathalocyanine composite materials also prepared by non-covalent $\pi - \pi$ stacking interactions and used for various applications [35]. C.-Y. Lin et al. have prepared poly(3,4-ethylenedioxythiophene)/FePc/MWCNT nanocomposite for the electrochemical oxidation of nitrite [36]. FePc modified MWCNT paste electrodes has been prepared for the selective determination of dopamine in the presence of serotonin [37]. K.I. Ozoemena et al. fabricated a novel electrochemical sensors based on carbon paste impregnated with iron and cobalt pthalocyanine for the determinaion of anti-HIV drug 2',3'-dideoxyinosine [38].

Herein we report the preperation of GO-CNT-FePc composite by simple sonication approach and demonstraed the modified electrode for the determination of hydrazine. The electrode preperation is very simple, reproducible and the proposed sensor shows very low detection limit of 9.3×10^{-8} M for the hydrazine determination.

2. EXPERIMENTAL

2.1 Reagents and materials

Hydrazine sulfate ($NH_2NH_2.H_2SO_4$) was purchased from Hayashi Pure chemical Industries Ltd, Japan and used as received. Graphite (powder, <20 μm), MWCNT (bundled > 95%, O.D × I.D × length of 7-15 nm × 3-6 nm × 0.5-200 μm) and all other chemicals were purchased from Aldrich. All

the reagents used were of analytical grade and used as received. The supporting electrolyte used for electrochemical studies was 0.05 M Phosphate buffer solution (PBS), prepared using Na_2HPO_4 and NaH_2PO_4 and the pH was adjusted either using H_2SO_4 or NaOH. Double distilled water (conductivity ≥ 18 MΩ) was used for all the experiments.

2.2 Apparatus

The electrochemical measurements were carried out using CHI 611a work station with a conventional three electrode cell using BAS GCE as working electrode (area 0.0706 cm^2), Ag|AgCl (sat. KCl) as reference electrode and Pt wire as counter electrode. Prior to each experiment, all the solutions were deoxygenated by passing pre-purified N_2 gas for 15 min. The supporting electrolyte used for electrochemical studies was 0.05 M PBS (pH 7). Amperometric (i-t curve) measurements were performed with analytical rotator AFMSRX (PINE instruments, USA) with a rotating disc electrode (RDE) having working area of 0.24 cm^2. EIM6ex ZAHNER (Kroanch, Germany) was used for electrochemical impedance spectroscopy (EIS) studies. Scanning electron microscopy (SEM) studies and transmission electron microscopy (TEM) have been performed with Hitachi S-3000 H scanning electron microscope and Hitachi H-7000 respectively. Energy-dispersive X-ray (EDX) spectra was recorded using HORIBA EMAX X-ACT (Model 51-ADD0009, Sensor + 24V=16 W, resolution at 5.9 keV = 129 eV).

2.3. Preparation of GO-CNT-FePc modified GCE

GO dispersed CNT was prepared in accordance with our previous report [32]. Afterwards, Iron phthalocyanine solution with the concentration of 0.5 mg mL^{-1} was prepared by dispersing in DMF with the aid of ultrasonication for 30 minutes. GO dispersed CNT (0.5 mg mL^{-1}) was mixed with equimolar ratio (1:1) of FePc solution (1 mg mL^{-1}) and stirred for 15 minutes. Then the mixture was ultrasonicated for 30 minutes to obtain GO-CNT-FePc composite.

GCE surface was polished with 0.05 μm alumina slurry using a Buehler polishing kit, then washed with water, ultrasonicated for 5 min and dried. 5 μl dispersion of GO-CNT-FePc composite was drop casted onto the pre-cleaned GCE and dried at room temperature. Then GO-CNT-FePc modified GCE (GO-CNT-FePc/GCE) was rinsed with water and used for the electrochemical studies. For comparison, GO-CNT and FePc modified GCEs were prepared by adopting the similar procedures.

3. RESULTS AND DISCUSSION

3.1 SEM and TEM Characterization of GO-CNT and GO-CNT-FePc

Fig. 1 shows the SEM images of GO-CNT composite (A), FePc (B) and GO-CNT-FePc composite (C). SEM image of GO-CNT depicts the typical morphology of GO-CNT composite with wrinkled GO sheets wrapped around the CNTs. In our previous report, we proved that a non-covalent

$\pi-\pi$ stacking interaction is operating between hydrophobic domain of the GO sheets and sidewalls of the CNTs [32]. SEM image of FePc depicts the typical grain like particle morphology of the phthalocyanine compounds [39].
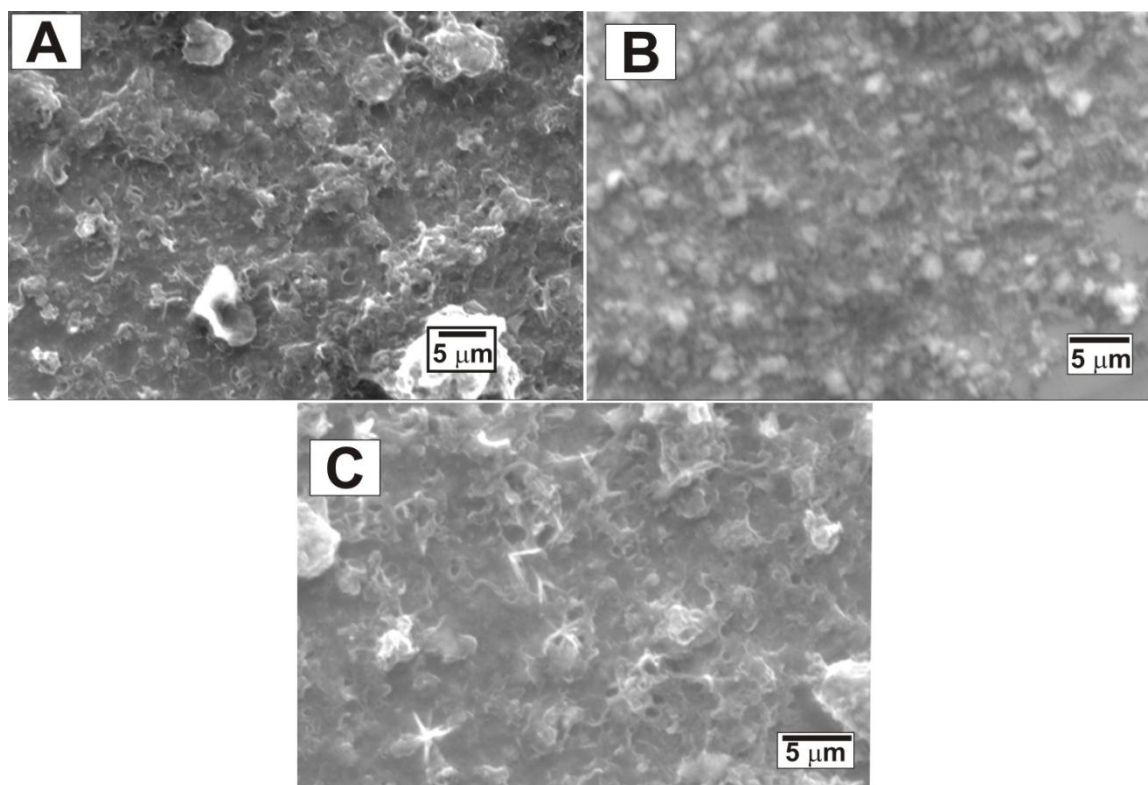

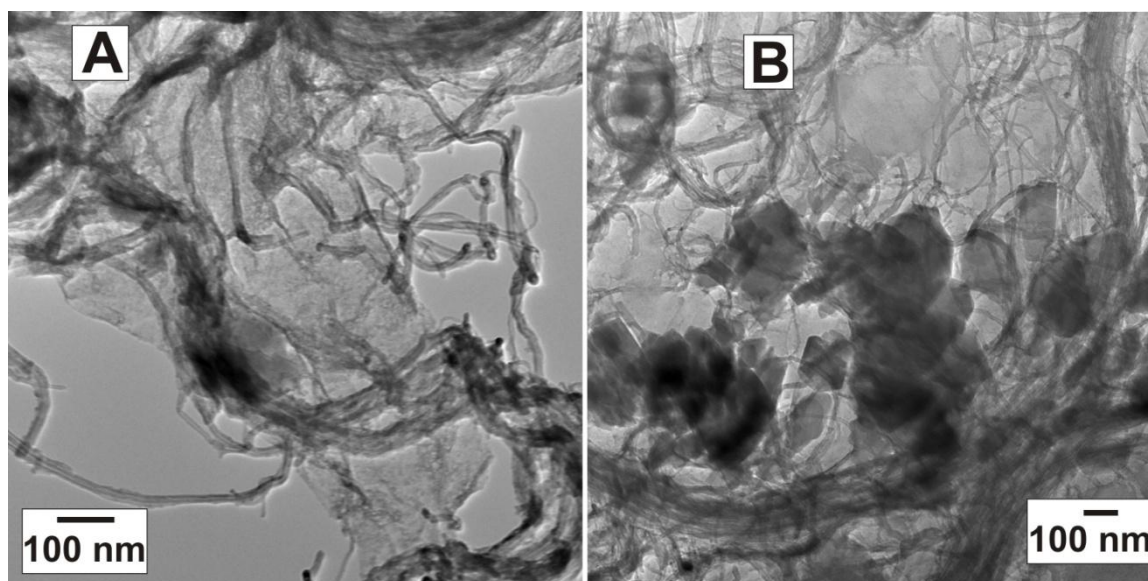**Figure 1.** SEM images of GO-CNT (A), FePc (B) and GO-CNT-FePc composite (C).

Figure 2. TEM image of GO-CNT composite (A) and GO-CNT-FePc composite (B).

Whereas SEM image of GO-CNT-FePc depicts a different morphology of cluster and layer like image with more porous and active sites onto the surface. This different morphology indirectly proves the formation of GO-CNT-FePc composite.

TEM image of the GO-CNT composite clearly shows that carbon nanotubes were completely covered by the GO sheets through π–π stacking interactions. TEM image of GO-CNT-FePc depicts that FePc molecules were randomly arranged as particles inside the GO-CNT composite networks. Thus, both SEM and TEM morphological studies proved that GO-CNT-FePc composite has been formed.

3.2 EDX characterization

EDX spectra have been used for the elemental characterization of the prepared composite. EDX spectrum of GO-CNT shows the presence of signals for carbon and oxygen with carbon weight percentage of 72.43 % and oxygen weight percentage of 27.57 %. The presence of oxygen content reveals the association of GO along with CNT as a GO-CNT composite; since the source of oxygen is only form GO.
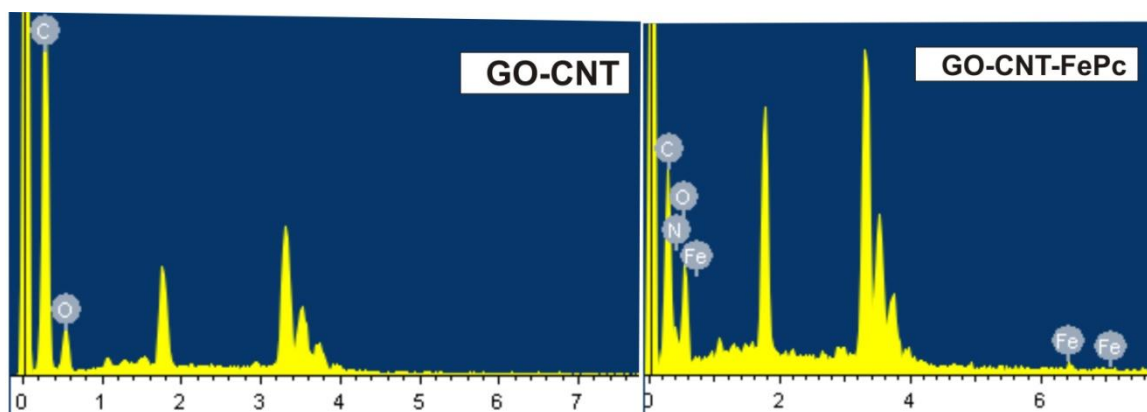

Figure 3. EDX spectra of GO-CNT and GO-CNT-FePc composite**.**

Interestingly, GO-CNT-FePc shows the presence of signals for C, O, N and Fe with weight percentage of 35.48, 20.44, 37.19 and 6.89 % respectively. The presence of signals for N and Fe in the GO-CNT-FePc composite clearly indicates that FePc molecules were strongly connected with GO-CNT composite. Hence EDX results also confirmed the formation of GO-CNT and GO-CNT-FePc composite.

3.3 EIS Characterization of the modified electrodes

EIS is an efficient tool to monitor the double layer capacitance and interfacial properties of the modified electrodes. Fig. 4 depicts the real and imaginary parts of the EIS represented as Nyquist plots

(Zim vs. Zre) for bare (a), GO-CNT (b), FePc (c) and GO-CNT-FePc (d) modified GCEs in pH 7 PBS containing 5 mM $Fe(CN)_6^{3-}/Fe(CN)_6^{4-}$. In comparison with EIS of bare GCE, the EIS of GO-CNT modified GCE exhibits highly depressed semicircle with very low R_{et} (charge transfer resistance value), attributed to the high conductivity of the GO-CNT composite modified electrode.
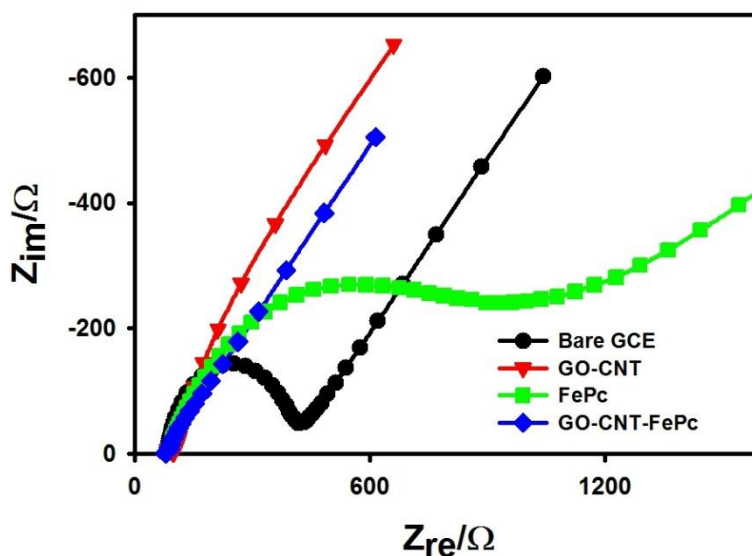

Figure 4. EIS of bare (a), GO-CNT (b), FePc (c) and GO-CNT-FePc (d) modified GCEs in 5mM $Fe(CN)_6^{3-}/Fe(CN)_6^{4-}$ in PBS (pH 7). Applied AC voltage: 5 mV, frequency: 0.1 Hz to 100 kHz.

EIS of FePc modified GCE exhibits a semicircle of larger diameter with higher R_{et}. On the other hand, after its incorporation with GO-CNT composite as a GO-CNT-FePc composite the semicircle becomes smaller with very low R_{et}. This could be due to the facile interaction between GO-CNT composite and FePc, which facilitates the excellent conductivity of the modified film. Thus, EIS results shows that the R_{et} value of the various modified electrodes were different, which makes a way to characterize the modified electrodes and proves that GO-CNT-FePc has been formed with very good interaction between GO-CNT and FePc.

3.4 Electrocatalytic oxidation of hydrazine

The various modified electrodes were electrochemically characterized by cyclic voltammetry. Fig. 5A shows cyclic voltammograms (CVs) of unmodified (a), FePc (b), GO-CNT (c) and GO-CNT-FePc (d) composite film modified GCEs in PBS (pH 7) at a scan rate of 50 mVs^{-1}. It is evident that bare GCE and FePc modified GCE exhibits very small background currents compared with the other modified films. GO-CNT composite exhibits enhanced background currents due to the presence of highly conductive CNT, though it comprises insulating GO. Whereas, GO-CNT-FePc shows one obvious reversible redox peaks centered at +0.176 V and one quasi reversible peak centered at -0.056 V. From the previous literature, it was known that the redox peak appeared at +0.176 in the composite, is due to the one electron redox reaction involving iron and phthalocyanine [Fe(III)Pc(-2)]$^+$/Fe(II)Pc(-

2) [40]. It is important to note that pristine FePc alone does not show any obvious redox peaks, whereas it shows well defined and obvious redox peaks after its incorporation with GO-CNT. This could be ascribed to the strong affinity interaction of FePc with the GO-CNT composite, which facilitates the enhanced redox peaks.
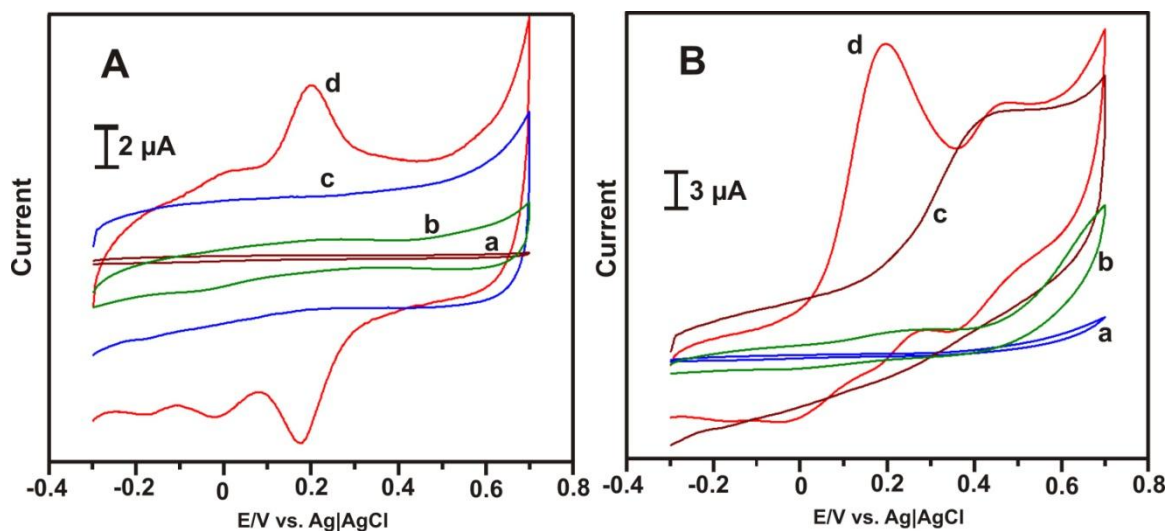

Figure 5. A) CVs of bare GCE (a) FePc, (b), GO-CNT(c) and GO-CNT-FePc (d) modified GCEs in PBS (pH 7) at the scan rate of 50 mVs^{-1}. B) CVs for the electrocatalysis of 0.5 mM of hydrazine in PBS (pH 7) at bare GCE (a), FePc (b), GO-CNT(c) and GO-CNT-FePc (d).

Fig. 5B shows the CVs towards electro-oxidation of 0.5 mM of hydrazine in PBS (pH 7) at bare GCE (a), FePc (b), GO-CNT(c) and GO-CNT-FePc (d) modified GCEs. It can be seen from the figure that bare GCE does not show any obvious peak for the oxidation of hydrazine observed in the entire electrochemical window used. FePc modified GCE shows very small anodic response, though the overpotential has been significantly reduced to +0.25 V. GO-CNT modified GCE shows enhanced electrocatalysis towards the oxidation of hydrazine at the potential of +0.43 V. On the other hand, GO-CNT-FePc exhibits a well obvious and greatly enhanced hydrazine oxidation peak current with great reduction of overpotential at +0.18V. In addition to this peak, GO-CNT-FePc exhibits one more electrocatalytic peak for the oxidation of hydrazine at +0.45 V, which is due to the catalytic ability of the CNT. The superior electrocatalytic performance of the GO-CNT-FePc towards the electrocatalysis of hydrazine compared with bare GCE and other modified electrodes could be ascribed to the excellent synergy between GO dispersed CNT and FePc, since either pristine CNT or pristine FePc does not shows good electrocatalytic performance towards the oxidation of hydrazine. Since the electrocatalytic peak at +0.18V is more obvious and greatly decreased in overpotential, we choose this peak to study the amperometric determination of hydrazine. The large decrease in the overpotential associated with significant increase in the peak current demonstrates the faster electron transfer of hydrazine oxidation onto the GO-CNT-FePc modified GCE.

3.5 Different scan rate study

Fig.6A shows the effect of scan rate (v) on GO-CNT-FePc modified GCE in the presence of 0.5 mM hydrazine in PBS (pH 7). From curves (a-j), it is obvious that anodic hydrazine oxidation peak observed at 0.18 V increased linearly with scan rates between (0.1 - 1 V s^{-1}) and moreover the anodic peak potential has a tendency to shift more positive values (from 0.31 to 0.44 V) with increasing scan rate. As shown in the inset of Fig. 6A, the catalytic hydrazine oxidation peak current (I_{pa}) increased linearly with v^{½}, indicating that the hydrazine oxidation process occurred at GO-CNT-FePc modified GCE is a diffusion-controlled electrocatalytic reaction [41].
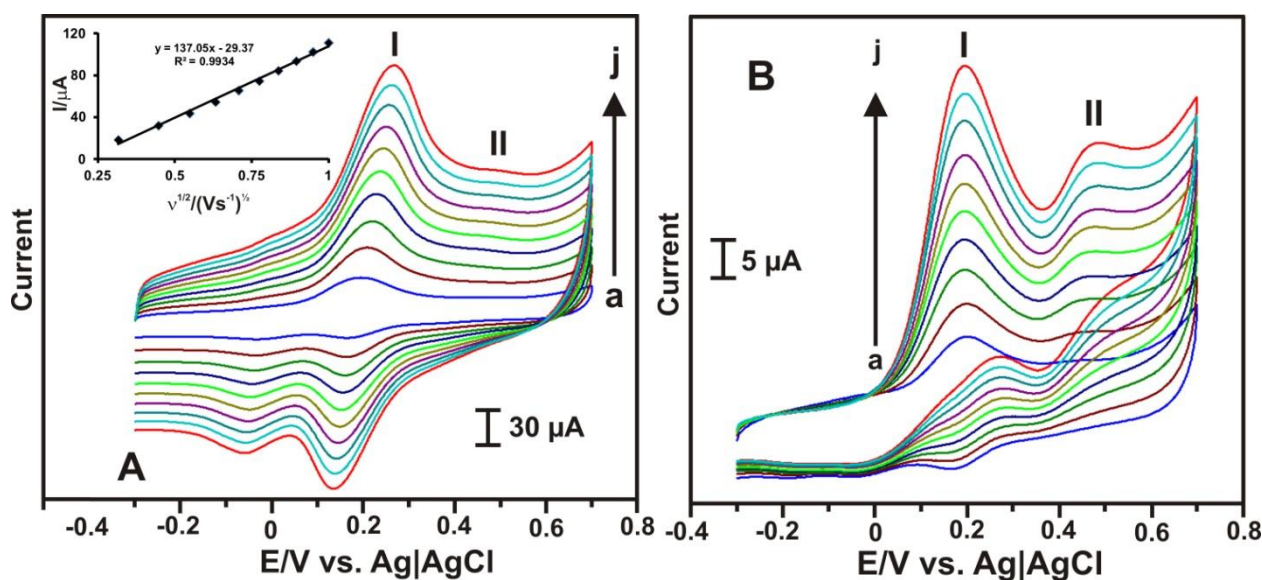

Figure 6. A) CVs of GO-CNT-FePc modified GCE in 0.1M PBS (pH 7) in presence of 0.5 mM of hydrazine, at different scan rates (from 0.1 to 1 Vs^{-1}). Inset: plot of square root of scan rate vs. peak current. (B) CVs of GO-CNT-FePc modified GCE in PBS (pH 7) in the presence of hydrazine ranging from 0.1 mM to 1 mM (a-j).

Fig. 6B shows the CVs of GO-CNT-FePc modified GCE in PBS (pH 7) in the presence of increasing concentration of hydrazine from 0.1 mM to 1 mM (a-j). It can be seen from the figure that both anodic catalytic peaks I and II are increasing consistently with the increasing concentrations of hydrazine. The linear increase in the peak current illustrates the excellent electrocatalytic ability of the modified electrode towards the oxidation of hydrazine. This result reveals that the GO-CNT-FePc modified GCE has great potential to catalyze the oxidation of hydrazine at significantly lower potential.

3.6 Amperometric determination of hydrazine at GO-CNT-FePc modified GCE

Fig. 7A displays the amperogram obtained at GO-CNT-FePc modified rotating disc GCE when each 0.5 µM hydrazine were injected sequentially into the continously stirred PBS (1600 RPM) at

regular intervals (50 s). During the amperometric experiments, +0.18 V was applied as the electrode potential (E_{app}). For every additon, a quick and well defined responses (with in 5 s) were observed. The amperometric response current increased linearly with increase in hydrazine concentrations between 5×10^{-7} - 8.35×10^{-5} M hydrazine (Fig. 7B).
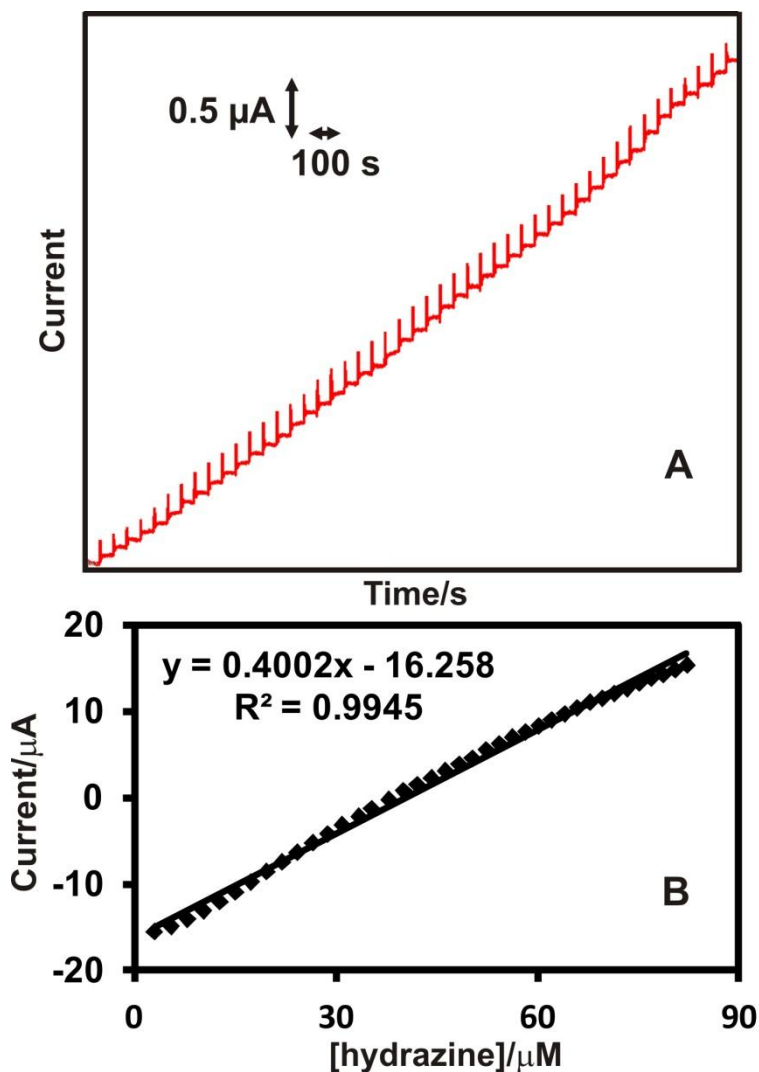

Figure 7. A) Amperometric i-t response obtained at GO-CNT-FePc modified rotating disc GCE upon successive additions of 0.5 µM hydrazine into continuously stirred PBS (pH 7). Rotation speed 1600 rpm; Eapp= +0.18 V. B) Calibration plot: [hydrazine] vs. peak current.

The linear regression equation has been expressed as Ip/µA =0.4002[hydrazine]/ µAµM^{-1} - 16.258; R^2 = 0.994 and sensitivity of the sensor is calculated to be 1.67 µA µM^{-1} cm^{-2}. The detection limit (LOD) was calculated using the well known formula, LOD = 3 s_b/S, where s_b is the standard deviation of the blank signal and S is the sensitivity [42]. The detection limit has been calculated to be 9.3×10^{-8} M. Low detection limit with wide working linear range shows that GO-CNT-FePc modified GCE can be used for the sensitive electrochemical determination of hydrazine.

The repeatability and reproducibility of the proposed sensor towards the determination of hydrazine has been performed by CV studies. CVs were recorded in PBS of pH 7 towards 0.5 mM hydrazine at the scan rate of 50 mVs^{-1}. The sensor exhibits acceptable repeatability with relative standard deviation (R.S.D) of 2.81 % for 8 successive measurements. Morover, it has a good reproducibility with an R.S.D of 3. 54 % for 5 individual measurements. Thus the proposed GO-CNT-FePc film based sensor showed acceptable repeatability and reproducibility for the electrochemical determination of hydrazine.

3.7 Real sample analysis

Real sample analysis were performed form water samples collected from various water sources such as river, tap and rain. Known amount of hydrazine were spiked into the collected water samples and the spiked water samples were analyzed using GO-CNT-FePc film modified GCE by amperometry adopting standard addition method. Amerpometry experiments were conducted under the similar experimental conditions as mentioned in section 3.6. The comparison of the spiked values and the determined values were listed in the Table 1.

Table 1. Determination of hydrazine in various water samples at GO-CNT-FePc film modified GCE

Samples	Added (μM)	Found (μM)	Recovery (%)
	10	10.25	102.5
Tap water	15	14.47	96.46
Rain water	10	9.76	97.6
	15	14.5	96.6
River water	10	10.33	103.3
	15	15.61	104.0

The added glucose shows the adequate recoveries from 96.6 to 104 %. The good recoveries achieved for hydrazine determination in the various water samples reveals the practical feasibility of the proposed GO-CNT-FePc film modified GCE.

4. CONCLUSIONS

A novel composite film GO-CNT-FePc has been synthesized by a simple sonication approach, Surface morphological studies and elemental analysis were proved the formation of GO-CNT-FePc

composite. The GO-CNT-FePc composite modified GCE has been demonstrated for the sensitive determination of hydrazine. The developed amperometric sensor shows excellent electrocatalytic activity towards oxidation of hydrazine and exhibits very low detection limit of 9.3×10^{-8} M with wide linear range. The high sensitivity, fast response and stable amperometric response reveal its scope for the other sensor applications. The proposed sensor detects hydrazine present in various water samples with good recoveries revealing its excellent practicallity.

References

1. S. Ameen, M.S. Akhtar, H.S. Shin, *Sens. Actuators, B*, 173 (2012) 177.
2. J.-X. Wei, A.P. Periasamy, S.-M. Chen, *Int. J. Electrochem. Sci.*, 6 (2011) 2411.
3. M.M. Ardakani, M.A. Karimi, M.M. Zare, S.M. Mirdehghan, *Int. J. Electrochem. Sci.,* 3 (2008) 246.
4. Y. Umasankar, T.-Y. Huang, S.-M. Chen, *Anal. Biochem.,* 408 (2011) 297.
5. S. Ganesh, F. Khan, M.K. Ahmed, S.K. Pandey, *Talanta,* 85 (2011) 958.
6. A. Safavi, M.A. Karimi, *Talanta,* 58 (2002) 785.
7. G.W. Watt, J.D. Chrisp, *Anal. Chem.* 24 (1952) 2006.
8. V. Mani, A.P. Periasamy, S.-M. Chen, *Electrochem. Commun.,* 17 (2012) 75.
9. X. Li, Z. Chen, Y. Zhong, F. Yang, J. Pan, Y. Liang, *Anal. Chim. Acta,* 710 (2012) 118.
10. C. Wang, L. Zhang, Z. Guo, J. Xu, H. Wang, K. Zhai, X. Zhuo, *Microchim. Acta,* 169 (2010) 1.
11. K.N. Han, C.A. Li, M.-P.N. Bui, X.-H. Pham, G. H. Seong, *Chem. Commun.,* 47 (2011) 938.
12. M.B. Gholivanda, A. Azadbakht, *Electrochim. Acta*, 56 (2011) 10044.
13. M. Hadi, A. Rouhollahi, M. Yousefi, *Sens. Actuators, B*, 160 (2011) 121.
14. S. Chakraborty, C.R. Raj, *Sens. Actuators, B,* 147 (2010) 222.
15. B. Unnikrishnan, S. Palanisamy, S.M. Chen, *Biosens. Bioelectron.*, 39 (2013) 70.
16. Y. Li, Y. Umasankar, S.M. Chen, *Talanta* 79 (2009) 486.
17. Y. Li, Y. Umasankar, S.M. Chen, *Anal. Biochem.* 388 (2009) 288.
18. Y. Umasankar, Y. Li, S.M. Chen, *J. Electrochem. Soc.* 157 (2010) K187.
19. A. P. Periasamy, Y. H. Ho, S. M. Chen, *Biosens. Bioelectron.*, 29(2011) 151.
20. S. Palanisamy, S. Cheemalapati, S.M. Chen, *Int. J. Electrochem. Sci.*, 7 (2012) 8394.
21. S. Palanisamy, S. Cheemalapati, S.M. Chen, *Anal. Biochem.* 429 (2012) 108.
22. S. Palanisamy, A.T. Ezhil Vilian, S. M. Chen, *Int. J. Electrochem. Sci..* 7(2012) 2153.
23. D.R. Dreyer, S. Park, C.W. Bielawski, R.S. Ruoff, *Chem. Soc. Rev.,* 39 (2010) 228.
24. L.J. Cote, F. Kim, J. Huang, *J. Am. Chem. Soc.,* 131 (2009) 1043.
25. C. Zhang, L. Ren, X. Wang, T. Liu, *J. Phys. Chem. C,* 114 (2010) 11435.
26. L. Qiu, X. Yang, X. Gou, W. Yang, Z.F. Ma, G.G. Wallace, D. Li, *Chem. Eur. J.,* 16 (2010) 10653.
27. M.-Y. Yen, M.-C. Hsiao, S.-H. Liao, P.-I Liu, H.-M. Tsai, C.-C.M. Ma, N.-W. Pu, M.-D. Ger, *Carbon,* 49 (2011) 3597.
28. X. Dong, G. Xing, M.B.C.-Park, W. Shi, N. Xiao, J. Wang, Q. Yan, T. C. Sum, W. Huang, P. Chen, *Carbon,* 49 (2011) 5071.
29. R.I. Jafri, T. Arockiados, N. Rajalakshmi, S. Ramaprabhua, J. Electrochem. Soc., 157 (2010) B874.
30. B. Devadas, V. Mani, S.-M. Chen, *Int. J. Electrochem. Sci.,* 7 (2012) 8064.
31. S. Woo, Y.-R. Kim, T.D. Chung, Y. Piao, H. Kim *Electrochim. Acta,* 59 (2012) 509.

32. V. Mani, B. Devadas, S.-M. Chen, *Biosens. Bioelectron.,* (2012), http://dx.doi.org/10.1016/j.bios.2012.08.045.
33. M. Siswana, K.I. Ozoemena, T.Nyokong, *Talanta,* 69 (2006) 1136.
34. G. Bottari, J.A. Suanzes, O. Trukhina, T. Torres, *J. Phys. Chem. Lett.,* 2 (2011) 905.
35. J. Yang, D. Mu, Y. Gao, J. Tan, A. Lu, D. Ma, *J. Nat. Gas Chem.,* 21 (2012) 265.
36. C.-Y. Lin, A. Balamurugana, Y.-H. Lai, K.-C. Ho, *Talanta,* 82 (2010) 1905.
37. D. Patrascu, I. David, V. David, C. Mihailciuc, I. Stamatin, J. Ciurea, L. Nagy, G.Nagy, A.A. Ciucu, *Sens. Actuators, B,* 156 (2011) 731.
38. K.I. Ozoemena, R.-I.S. Staden, T. Nyokong, *Electroanalysis,* 21 (2009) 1651.
39. P. Kalugasalam, Dr.S. Ganesan, *Int. J. Eng. Sci. tech.* 2 (2010) 1773.
40. Y. Yuan, B. Zhao, Y. Jeon, S. Zhong, S. Zhou, S. Kim, *Bioresour. Technol.,* 102 (2011) 5849.
41. W. Sultana, S. Ghosh, B. Eraiah, *Electroanalysis,* 24 (2012) 1869.
42. G.P. Keeley, A.O'Neill, M. Holzinger, S. Cosnier, J.N. Coleman, G.S. Duesberg, *Phys. Chem. Chem. Phys.,* 13 (2011) 7747.